

Exploiting Inter-Sample Correlation and Intra-Sample Redundancy for Partially Relevant Video Retrieval

Junlong Ren*
The Hong Kong University of Science
and Technology (Guangzhou)
Guangzhou, China
jren686@connect.hkust-gz.edu.cn

Gangjian Zhang*
The Hong Kong University of Science
and Technology (Guangzhou)
Guangzhou, China
gzhang292@connect.hkust-gz.edu.cn

Yu Hu
The Hong Kong University of Science
and Technology (Guangzhou)
Guangzhou, China
yhu847@connect.hkust-gz.edu.cn

Jian Shu
The Hong Kong University of Science
and Technology (Guangzhou)
Guangzhou, China
jshu704@connect.hkust-gz.edu.cn

Hao Wang[†]
The Hong Kong University of Science
and Technology (Guangzhou)
Guangzhou, China
haowang@hkust-gz.edu.cn

Abstract

Partially Relevant Video Retrieval (PRVR) aims to retrieve the target video that is partially relevant to the text query. The primary challenge in PRVR arises from the semantic asymmetry between textual and visual modalities, as videos often contain substantial content irrelevant to the query. Existing methods coarsely align paired videos and text queries to construct the semantic space, neglecting the critical cross-modal dual nature inherent in this task: inter-sample correlation and intra-sample redundancy. To this end, we propose a novel PRVR framework to systematically exploit these two characteristics. Our framework consists of three core modules. First, the Inter Correlation Enhancement (ICE) module captures inter-sample correlation by identifying semantically similar yet unpaired text queries and video moments, combining them to form pseudo-positive pairs for more robust semantic space construction. Second, the Intra Redundancy Mining (IRM) module mitigates intra-sample redundancy by mining redundant video moment features and treating them as hard negative samples, thereby encouraging the model to learn more discriminative representations. Finally, to reinforce these modules, we introduce the Temporal Coherence Prediction (TCP) module, which enhances feature discrimination by training the model to predict the original temporal order of randomly shuffled video frames and moments. Extensive experiments on three datasets demonstrate the superiority of our approach compared to previous methods, achieving state-of-the-art results.

CCS Concepts

• **Information systems** → **Multimedia and multimodal retrieval**; **Video search**.

Keywords

Cross-Modal Retrieval, Video Understanding, Multimodal Learning, Multimedia Applications

1 Introduction

With the explosion of online video content, users increasingly seek efficient ways to find specific videos within vast video collections.

*Equal contribution; [†]Corresponding author.

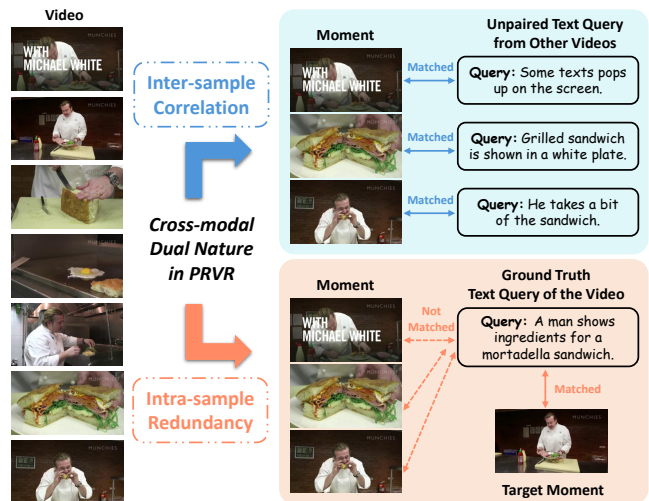


Figure 1: In Partially Relevant Video Retrieval (PRVR), video-text samples exhibit the inherent cross-modal dual nature: (a) Inter-sample correlation: The video contains certain moments that are semantically correlated to other unpaired text queries. (b) Intra-sample redundancy: Apart from the target moment, other redundant moments in the video are irrelevant to the paired text query.

While conventional video retrieval methods focus on identifying videos that fully match a given query, many real-world scenarios require identifying videos that contain only partial moments relevant to a user’s descriptive text query. This task is formally known as Partially Relevant Video Retrieval (PRVR).

The fundamental challenge in PRVR stems from the inherent semantics asymmetry between text and video modalities. While a video comprises multiple moments, only a subset may exhibit relevance to a given text query. Existing methods [8, 13, 19, 40, 44] approach this task from a limited perspective, primarily adopting conventional alignment constraints such as triplet ranking [14] and InfoNCE [33] to establish coarse associations between annotated paired text query and the target videos. These approaches may be effective when the semantic content of the two modalities is largely equivalent, as in the traditional text-to-video retrieval tasks.

However, these methods overlook the unique cross-modal dual nature in the PRVR task: namely inter-sample correlation and intra-sample redundancy. As illustrated in Figure 1, the video modality inherently shows richer semantics than the corresponding text query. Moments not explicitly related to the query may still contain valuable visual semantics that correlate with other unpaired queries in the dataset. Conversely, the video modality also suffers from semantic redundancy, as only a limited subset of its content aligns with the given textual descriptions [8]. This results in a substantial portion of video content being irrelevant to the text query, which may not only fail to contribute to retrieval accuracy but could actively hinder the proper alignment between text queries and their corresponding video moments.

Based on these observations, our approach aims to enhance PRVR by simultaneously leveraging inter-sample correlations and mitigating intra-sample redundancy. To harness inter-sample correlations, we propose to fully utilize the rich semantics presented in videos. Technically, our method identifies and exploits underlying semantic relationships between unpaired video moments and text queries within the training set. This approach stems from the key insight that while certain video moments may not directly correspond to their paired text descriptions, they often share meaningful semantic connections with other queries in the dataset. By establishing these additional cross-modal associations, we enhance the construction of a more robust and discriminative semantic space.

To address intra-sample redundancy, our framework explicitly mitigates the interference caused by irrelevant video moments in video-text matching. We propose to treat redundant moment features as hard negative samples during model training. These redundant features, while semantically distinct from the target moment, exhibit high similarity as they originate from the same video. By forcing the model to distinguish these challenging negative samples and true positive matches, we encourage the learning of more precise and discriminative visual representations that better align with their corresponding textual descriptions.

In this paper, we introduce a novel framework for PRVR that systematically exploits the cross-modal dual nature of video-text relationships through two key characteristics: inter-sample correlation and intra-sample redundancy. The proposed framework comprises three key components: **(1)** The Inter Correlation Enhancement module is designed to fully exploit the inter-sample correlation of video-text modalities. It computes the cross-modal similarity between video moments and unpaired text queries. High-similarity pairs are identified and utilized as pseudo-positive samples, which are then incorporated into the alignment objective to construct a more comprehensive and discriminative cross-modal embedding space. **(2)** To address intra-sample redundancy, the Intra Redundancy Mining module extracts semantically redundant video moments through joint analysis of text features, global video features, and local moment features. These redundant features serve as hard negative samples during training, forcing the model to strengthen alignment between text and relevant video content and improve discrimination against irrelevant visual semantics within the same video. **(3)** Complementing the above modules, the Temporal Coherence Prediction module enhances temporal feature discrimination through an auxiliary self-supervised task. The model learns to predict the original temporal order of randomly

shuffled video frames/moments, thereby developing a more robust understanding of video semantics and temporal structure.

Extensive experiments on three large-scale datasets, TVR [24], ActivityNet Captions [22], and Charades-STA [16], verify the superior performance and robustness of our proposed method. In summary, our principal contributions are summarized as follows:

- We introduce the Inter Correlation Enhancement module, which identifies high-similarity pairs between video moments and unpaired text queries. These pseudo-positive pairs are incorporated to enrich the cross-modal semantic space construction.
- We propose the Intra Redundancy Mining module to extract and leverage redundant video moment features as hard negative samples. It forces the model to develop more precise text-video alignment by distinguishing relevant semantics from redundant visual content within the same video.
- In the Temporal Coherence Prediction module, we design a self-supervised auxiliary task. It enhances temporal feature discrimination by requiring the model to predict the original temporal order of shuffled video frames/moments. This results in more robust and discriminative video features.

2 Related Work

2.1 Partially Relevant Video Retrieval

Partially Relevant Video Retrieval (PRVR) is to retrieve untrimmed videos that are only partially semantically related to the text query. Unlike previous video retrieval tasks, videos retrieved by PRVR do not necessarily exhibit complete semantic alignment with the textual query, often containing substantial redundant information. Specifically, MS-SL [8] is the first to propose the PRVR task. MS-SL learns video features at both the clip-scale and frame-scale. PEAN [19] introduces a Gaussian-based pooling strategy to improve the model’s holistic understanding of events. DL-DKD [13] distills CLIP’s [34] prior knowledge of image-text matching and mitigates the domain gap. GMMFormer [40] increases information density in video encoding by adopting Gaussian windows in Transformer blocks [37]. BGM-Net [44] proposes a new loss function to facilitate multimodal alignment based on unimodal similarities. However, these works neglect the unique cross-modal dual nature in PRVR, leading to limited semantic space construction. In contrast, we aim to exploit the inter-sample correlation and intra-sample redundancy, resulting in improved retrieval accuracy.

2.2 Video Moment Retrieval

Video Moment Retrieval (VMR) aims to extract the start/end time boundaries of semantically relevant moments from an untrimmed video with text queries. Existing methods can be generally classified into proposal-based [15, 28, 41, 45, 48, 49] and proposal-free [11, 17, 31, 47, 50, 51] approaches. Proposal-based methods first generate a set of candidate moment proposals and subsequently identify the best-matching proposal. In contrast, proposal-free methods directly predict the start and end timestamps by integrating video and query features, thus eliminating the need for explicit proposals. Departing from these conventional methods, recent studies [2, 20, 23, 27, 29, 32] also utilize the architecture of DETR [3] to address VMR as a set prediction task. Unlike VMR, PRVR focuses on retrieving

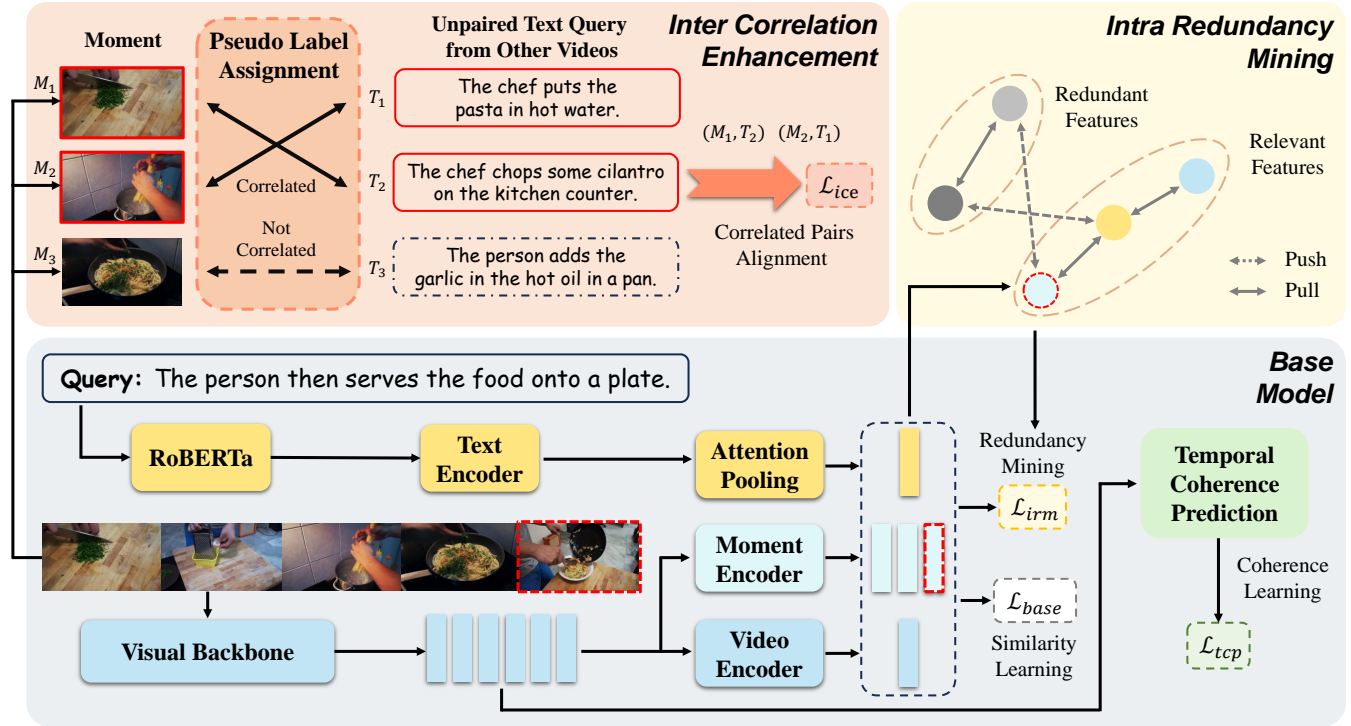


Figure 2: Overview of the proposed framework. We systematically leverage the cross-modal dual nature in PRVR, namely inter-sample correlation and intra-sample redundancy, to construct a more discriminative cross-modal semantic space. The framework comprises three key components: (a) **Inter Correlation Enhancement Module**: This component analyzes cross-modal correlations by identifying high-similarity pairs between video moments and unpaired text queries. These pseudo-positive pairs are incorporated during training to enrich the semantic space construction. (b) **Intra Redundancy Mining Module**: The module extracts and utilizes redundant video moments as hard negative samples. By learning to distinguish these hard negatives, the model develops enhanced capability to focus on query-relevant visual semantics. (c) **Temporal Coherence Prediction Module**: Designed to complement the other components, this module improves visual feature discrimination through a self-supervised sequence prediction task, where the model predicts the original temporal order of shuffled video frames/moments.

untrimmed videos instead of temporal locations of moments, thus the temporal annotations are not provided in PRVR.

2.3 Text-to-Video Retrieval

In recent years, Text-to-Video Retrieval (T2VR) has attracted increasing attention. A common approach [6, 9, 10, 12, 26] involves retrieving pre-trimmed videos by comparing cross-modal similarities between textual queries and video content. To achieve this, many studies [25, 39, 42] have proposed methods that project features from different modalities into a shared embedding space. However, these approaches often neglect the fact that real-world videos may not consistently correspond to a single topic, and typically certain all moments within a video are relevant to the textual query.

3 Proposed Method

In this section, we elaborate on the technical details of our proposed framework, which is illustrated in Figure 2. We first delineate the problem formulation in Section 3.1. Then the base model architecture is expounded in Section 3.2. The three key modules, namely Inter Correlation Enhancement module (ICE), Intra Redundancy Mining module (IRM), and Temporal Coherence Prediction module

(TCP) are presented in Section 3.3, Section 3.4, and Section 3.5, respectively. Finally, the training objective and model inference are detailed in Section 3.6.

3.1 Problem Formulation

Partially relevant video retrieval (PRVR) aims to retrieve videos containing a moment semantically relevant to a textual query, from a large corpus of untrimmed videos. Unlike conventional text-to-video retrieval, the videos are untrimmed and much longer, and text queries typically correspond to a small portion of a video. Note that the start/end timestamps of moments are unavailable in PRVR.

3.2 Base Model

3.2.1 Text Representation. Given a sentence containing N words, following previous works [8, 40, 44], we first employ the pre-trained RoBERTa [30] to extract word embeddings. Then we utilize a fully-connected (FC) layer to project the word embeddings into a lower-dimensional space. We further adopt a standard Transformer layer [37] as the text encoder. The encoded word-level features are denoted as $Q = \{q_i\}_{i=1}^N \in \mathbb{R}^{N \times D}$, where D is the feature dimension. Finally, we apply the additive attention mechanism [1] on Q to

obtain the aggregated sentence-level feature $q \in \mathbb{R}^D$:

$$\alpha^q = \text{Softmax}(w^q \cdot Q^\top) \in \mathbb{R}^{1 \times N}, \quad q = \sum_{i=1}^N \alpha_i^q \times q_i, \quad (1)$$

where $w^q \in \mathbb{R}^{1 \times D}$ is a learnable weight.

3.2.2 Video Representation. Given an untrimmed video, we first adopt a pre-trained 2D or 3D CNN [4] as the visual backbone to extract T_f frame features. Following previous methods [8, 19, 40, 44], we employ a coarse-to-fine manner to capture the temporal information of videos by two distinct branches. Technically, the moment-level branch measures the local moment-text similarity while the video-level branch models the global video-text similarity.

For the moment-level branch, we first condense the T_f frame features into T_m moment features by mean pooling over consecutive frame features. We then use an FC layer to reduce dimension. For the moment encoder, a standard Transformer encoder [37] is adopted to get contextual moment features $V_m = \{m_i\}_{i=1}^{T_m} \in \mathbb{R}^{T_m \times D}$.

For the video-level branch, the frame features are fed into an FC layer, followed by the video encoder, which is a standard Transformer encoder. The encoded frame features are denoted as $V_f = \{f_i\}_{i=1}^{T_f} \in \mathbb{R}^{T_f \times D}$. Next, we employ the additive attention mechanism [1] on V_f to obtain the aggregated video-level feature $v \in \mathbb{R}^D$:

$$\alpha^v = \text{Softmax}(w^v \cdot V_f^\top) \in \mathbb{R}^{1 \times T_f}, \quad v = \sum_{i=1}^{T_f} \alpha_i^v \times f_i, \quad (2)$$

where $w^v \in \mathbb{R}^{1 \times D}$ is a learnable weight.

3.2.3 Similarity Learning. Given a video-text pair \mathcal{V} and \mathcal{T} , we first compute the similarity between the text representation and video representations from the two aforementioned branches. Concretely, the video-level similarity between the video feature v and the sentence feature q is measured by the cosine similarity:

$$S_v(\mathcal{V}, \mathcal{T}) = \cos(v, q) = \frac{v^\top q}{\|v\| \cdot \|q\|}. \quad (3)$$

Next, we compute the moment-level similarity between moment features V_m and the sentence feature q through the max-pooling operation and identify the target moment feature $m^t \in \mathbb{R}^D$:

$$S_m(\mathcal{V}, \mathcal{T}) = \max\{\cos(m_1, q), \dots, \cos(m_{T_m}, q)\} = \cos(m^t, q). \quad (4)$$

For training, we adopt the triplet ranking [14] and InfoNCE [33] losses, which is a common approach following [8, 13, 19, 40, 44]:

$$\mathcal{L}^{trip} = \frac{1}{n} \sum_{(\mathcal{V}, \mathcal{T}) \in \mathcal{B}} [\max(0, m + S(\mathcal{V}, \mathcal{T}^-) - S(\mathcal{V}, \mathcal{T})) + \max(0, m + S(\mathcal{V}^-, \mathcal{T}) - S(\mathcal{V}, \mathcal{T}))], \quad (5)$$

$$\mathcal{L}^{nce} = -\frac{1}{n} \sum_{(\mathcal{V}, \mathcal{T}) \in \mathcal{B}} \left[\log \left(\frac{S(\mathcal{V}, \mathcal{T})}{\sum_{\mathcal{T}_i} S(\mathcal{V}, \mathcal{T}_i)} \right) + \log \left(\frac{S(\mathcal{V}, \mathcal{T})}{\sum_{\mathcal{V}_i} S(\mathcal{V}_i, \mathcal{T})} \right) \right], \quad (6)$$

where m is the margin constant, n is the size of the mini-batch \mathcal{B} , \mathcal{T}^- and \mathcal{V}^- are negative samples from \mathcal{B} , \mathcal{T}_i and \mathcal{V}_i denote all text and video samples. The training loss of the base model is:

$$\mathcal{L}_{base} = \mathcal{L}_v^{trip} + \mathcal{L}_m^{trip} + \lambda_1 \mathcal{L}_v^{nce} + \lambda_2 \mathcal{L}_m^{nce}, \quad (7)$$

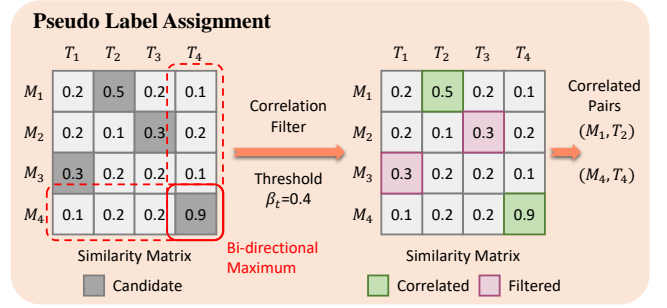


Figure 3: The ICE module employs a two-stage selection process for pseudo label assignment. It first computes the similarity between unpaired video moments and text features in a mini-batch. The pairs with mutual maximum similarity are selected as candidate pairs. Then, only those pairs with a similarity higher than the threshold are retained, ensuring high-confidence pseudo labels for subsequent training.

where \mathcal{L}_v^{trip} and \mathcal{L}_m^{trip} denote triplet losses using the video-level similarity S_v and moment-level similarity S_m as S , and accordingly for \mathcal{L}_v^{nce} and \mathcal{L}_m^{nce} . λ_1 and λ_2 are hyperparameters to balance losses.

3.3 Inter Correlation Enhancement

The PRVR task presents a fundamental semantic asymmetry, where textual queries only partially describe the content of target videos, leaving the visual modality inherently richer in semantic information. Our key observation reveals that while certain video moments may not align with their originally paired text annotations, they may exhibit strong semantic correspondence with other unpaired textual descriptions in the dataset as shown in Figure 1. This inter-sample correlation represents a valuable but underutilized resource in current PRVR approaches. We propose to exploit these underlying cross-modal relationships.

To achieve this, we propose the Inter Correlation Enhancement (ICE) module. Technically, we aim to additionally learn these unlabeled but correlated visual-text relationships, thus constructing a richer semantic space. We focus on exploiting moment-text pairs that are most likely to be semantically corresponding while filtering out those semantically irrelevant ones. The pseudo label assignment process is shown in Figure 3.

Given a mini-batch with n video-text pairs, we first extract text and moment features as defined in Section 3.2. This results in $n_m = nT_m$ moment features and n text features. Then, we calculate a similarity matrix $S = \{s_{ij}\} \in \mathbb{R}^{n_m \times n}$ for each moment feature and text feature. Note that we manually set the similarities between each text and moments from its paired video to -1 as we aim to mine unpaired correlated moment-text pairs. For the \bar{i} -th moment and \bar{j} -th text, we find the most similar text and moment, respectively:

$$\hat{j} = \arg \max_{j \in \{1, \dots, n\}} (\{s_{i\bar{j}}\}), \quad \hat{i} = \arg \max_{i \in \{1, \dots, n_m\}} (\{s_{i\bar{j}}\}), \quad (8)$$

if $\hat{i} = \bar{i}$ and $\hat{j} = \bar{j}$, they are mutually the most similar to each other and we deem them as a candidate correlated pair.

Intuitively, a truly correlated pair should not only mutually be the most similar to each other, but also exhibit high similarity. To

further filter out mismatched noisy pairs, we pre-define β_t as the correlation threshold. Only the pairs with a similarity higher than β_t are selected.

Finally, we obtain n_c correlated pairs through the above two-stage selection. These pairs then form a mini-batch of size n_c and we align them using contrastive learning losses defined in Equation (5) and (6). The loss of ICE is denoted as \mathcal{L}_{ice} .

3.4 Intra Redundancy Mining

The ICE module effectively harnesses inter-sample correlations to enhance the cross-modal semantic space for retrieval. However, while certain video semantics may align with unpaired text queries, they represent redundant information with respect to the originally paired text. This redundancy can introduce noise during video-text matching, thereby compromising retrieval accuracy.

To mitigate the intra-sample redundancy, we propose the Intra Redundancy Mining (IRM) module, which identifies redundant video moments by analyzing relationships among text, video, and moment-level features. These redundant features are then employed as hard negative samples during training. Unlike conventional negative samples (e.g., randomly sampled unpaired videos), these mined negatives exhibit higher feature similarity to the target moment, presenting a more challenging discrimination task. By forcing the model to distinguish these hard negatives, we promote the learning of more discriminative and query-relevant video representations, improving retrieval performance.

We construct redundant video features from two different perspectives. Technically, we model the semantic variation between the target moment feature m^t , video feature v , and query feature q to obtain the video-view redundant feature $r_v \in \mathbb{R}^D$ and query-view redundant feature $r_q \in \mathbb{R}^D$:

$$r_v = FC(v - m^t), r_q = FC(v - q), \quad (9)$$

where FC is a fully-connected layer to bridge the gap between video-moment and video-query differences. The intuition is that the video-level feature v contains global semantics of all moments within the video. By subtracting the target moment feature m^t from the video-level feature v , we obtain the video-view redundant feature r_v which is irrelevant to the text. Similarly, we use a symmetrical operation to obtain the query-view redundant feature r_q which is regarded to be irrelevant to the target moment. Since both redundant features r_v and r_q should be semantically irrelevant to the target moment feature and query feature, we employ r_v and r_q as negative samples in the moment-level similarity learning (Section 3.2.3), where the loss function is denoted as \mathcal{L}_{neg} .

Moreover, we further propose to directly align r_v and r_q . As the two redundant features are obtained at the video-view and query-view respectively, their alignment boosts the learning of underlying relationships between videos and text queries in the cross-modal semantic space. The corresponding loss \mathcal{L}_{red} is also the jointly application of Equation (5) and (6). The overall training objective of this module is the sum of the above two losses:

$$\mathcal{L}_{irm} = \mathcal{L}_{neg} + \mathcal{L}_{red}. \quad (10)$$

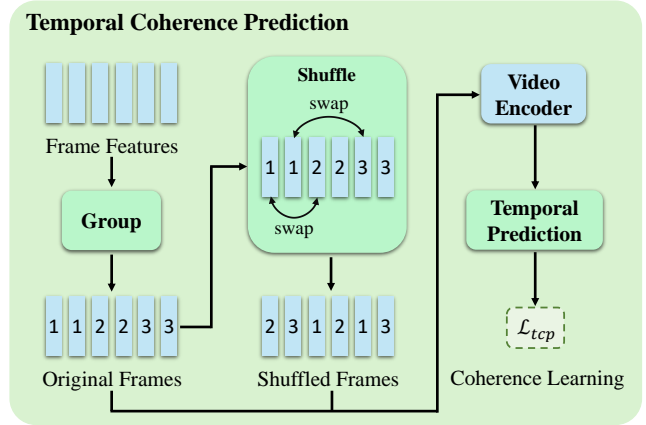


Figure 4: The pipeline of the Temporal Coherence Prediction (TCP) module. The frame features are first divided into distinct groups, and group labels are assigned accordingly. Then, a subset of frame features is randomly selected and shuffled, and the group labels with these frames are predicted.

3.5 Temporal Coherence Prediction

While our ICE and IRM modules effectively leverage inter-sample correlations and mitigate intra-sample redundancy, their performance fundamentally depends on the model’s ability to discern discriminative video features. Clearer feature distinctions enable more accurate cross-modal correlation measurement in ICE and better redundancy identification in IRM. To further enhance these capabilities, we introduce the Temporal Coherence Prediction (TCP) module, which strengthens temporal feature understanding through self-supervised learning. The pipeline is shown in Figure 4.

Specifically, the TCP module incorporates an auxiliary sequence prediction task. To capture the temporal structure of videos, we leverage the continuity between adjacent frames to partition the video sequence into coherent temporal segments. We group the video features and shuffle them to form an unordered sequence. The model is trained to predict the original temporal order. By explicitly modeling temporal coherence, this task helps the model to learn the coherence and causality between video events. Note that this strategy is applied to both the video-level branch and moment-level branch in Section 3.2.2 to enable multi-grained temporal coherence learning. We mainly take the video-level branch for explanation.

Concretely, we first group frame features into g groups and each frame feature is given its group label ranging from 1 to g . Every T_f/g consecutive frame features are assigned with the same group label. Group labels of the original encoded frame features V_f are denoted as $y_o \in \mathbb{R}^{T_f}$. We then randomly select and shuffle some frame features and encode them through the video encoder. Note that shuffling a small or large length of frames might lead to suboptimal performance. Too few shuffled frames provide insufficient learning signals, while excessive shuffling disrupts temporal coherence and makes the task overly challenging. Therefore, we pre-define β_r as the shuffle ratio. The shuffled frame features and their shuffled group labels are represented as $\hat{V}_f = \{\hat{f}_i\}_{i=1}^{T_f} \in \mathbb{R}^{T_f \times D}$ and $y_s \in \mathbb{R}^{T_f}$, respectively. Then we adopt a classifier to predict the group labels

Table 1: Comparison results on TVR, ActivityNet Captions, and Charades-STA. The best results are highlighted in bold, while the second-best outcomes are underlined. We achieve state-of-the-art results on all of the three datasets across all metrics.

Method	Venue	TVR					ActivityNet Captions					Charades-STA				
		R@1	R@5	R@10	R@100	SumR	R@1	R@5	R@10	R@100	SumR	R@1	R@5	R@10	R@100	SumR
HGR [6]	CVPR'2020	1.7	4.9	8.3	35.2	50.1	4.0	15.0	24.8	63.2	107.0	1.2	3.8	7.3	33.4	45.7
W2VV+ [26]	MM'2019	5.0	14.7	21.7	61.8	103.2	5.4	18.7	29.7	68.8	122.6	0.9	3.5	6.6	34.3	45.3
DE [9]	CVPR'2019	7.6	20.1	28.1	67.6	123.4	5.6	18.8	29.4	67.8	121.7	1.5	5.7	9.5	36.9	53.7
DE++ [10]	TPAMI'2021	8.8	21.9	30.2	67.4	128.3	5.3	18.4	29.2	68.0	121.0	1.7	5.6	9.6	37.1	54.1
RIVRL [12]	TCSVT'2022	9.4	23.4	32.2	70.6	135.6	5.2	18.0	28.2	66.4	117.8	1.6	5.6	9.4	37.7	54.3
Cap4Video [42]	CVPR'2023	10.3	26.4	36.8	74.0	147.5	6.3	20.4	30.9	72.6	130.2	1.9	6.7	11.3	45.0	65.0
XML [24]	ECCV'2020	10.0	26.5	37.3	81.3	155.1	5.3	19.4	30.6	73.1	128.4	1.6	6.0	10.1	46.9	64.6
ReLoCLNet [46]	SIGIR'2021	10.7	28.1	38.1	80.3	157.1	5.7	18.9	30.0	72.0	126.6	1.2	5.4	10.0	45.6	62.3
CONQUER [18]	MM'2021	11.0	28.9	39.6	81.3	160.8	6.5	20.4	31.8	74.3	133.1	1.8	6.3	10.3	47.5	66.0
MS-SL [8]	MM'2022	13.5	32.1	43.4	83.4	172.4	7.1	22.5	34.7	75.8	140.1	1.8	7.1	11.8	47.7	68.4
JSG [7]	MM'2023	-	-	-	-	-	6.8	22.7	34.8	76.1	140.5	2.4	7.7	12.8	49.8	72.7
UMT-L [25]	ICCV'2023	13.7	32.3	43.7	83.7	173.4	6.9	22.6	35.1	76.2	140.8	1.9	7.4	12.1	48.2	69.6
PEAN [19]	ICME'2023	13.5	32.8	44.1	83.9	174.2	7.4	23.0	35.5	75.9	141.8	<u>2.7</u>	<u>8.1</u>	<u>13.5</u>	50.3	<u>74.7</u>
InternVideo2 [39]	ECCV'2024	13.8	32.9	44.4	84.2	175.3	7.5	23.4	36.1	76.5	143.5	1.9	7.5	12.3	49.2	70.9
GMMFormer [40]	AAAI'2024	13.9	33.3	44.5	84.9	176.6	<u>8.3</u>	24.9	36.7	76.1	146.0	2.1	7.8	12.5	<u>50.6</u>	72.9
BGM-Net [44]	TOMM'2024	14.1	34.7	<u>45.9</u>	<u>85.2</u>	<u>179.9</u>	7.2	23.8	36.0	76.9	143.9	1.9	7.4	12.2	50.1	71.6
DL-DKD [13]	ICCV'2023	<u>14.4</u>	<u>34.9</u>	45.8	84.9	<u>179.9</u>	8.0	<u>25.0</u>	<u>37.5</u>	<u>77.1</u>	<u>147.6</u>	-	-	-	-	-
Ours	-	17.5	39.0	49.9	87.6	194.0	10.1	28.6	41.9	79.8	160.4	2.9	9.2	14.9	54.3	81.3

of both the original and shuffled frame features V_f and \hat{V}_f :

$$p_o = \text{Softmax}(\text{CLS}(V_f)), p_s = \text{Softmax}(\text{CLS}(\hat{V}_f)), \quad (11)$$

where CLS is a linear classifier, $p_o \in \mathbb{R}^{T_f \times g}$ and $p_s \in \mathbb{R}^{T_f \times g}$ are the predicted probability distributions of group labels. We adopt the cross-entropy loss to optimize this module:

$$\mathcal{L}_{tcp} = f_{CE}(p_o, y_o) + f_{CE}(p_s, y_s), \quad (12)$$

where f_{CE} represents the cross-entropy loss function.

3.6 Training and Inference

Our proposed method is optimized by the loss of each module:

$$\mathcal{L} = \mathcal{L}_{base} + \lambda_3 \mathcal{L}_{ice} + \lambda_4 \mathcal{L}_{irm} + \lambda_5 \mathcal{L}_{tcp}, \quad (13)$$

where λ_3 , λ_4 , and λ_5 are hyperparameters to balance losses.

During inference, the similarity of the given video-text pair \mathcal{V} and \mathcal{T} is the weighted sum of moment-level and video-level similarities following [8, 13, 19, 40, 44]:

$$\mathcal{S}(\mathcal{V}, \mathcal{T}) = \alpha \mathcal{S}_m(\mathcal{V}, \mathcal{T}) + (1 - \alpha) \mathcal{S}_v(\mathcal{V}, \mathcal{T}), \quad (14)$$

where $\alpha \in [0, 1]$ is a hyperparameter to balance the similarities.

4 Experiments

4.1 Experimental Setup

4.1.1 Datasets. To evaluate the effectiveness of our method on the PRVR task, we utilize three untrimmed video datasets: TVR [24], ActivityNet Captions [22], and Charades-STA [16]. Note that we do not use moment-level annotations provided by these datasets in the setting of PRVR. Unlike conventional T2VR datasets [5, 38, 43] using pre-trimmed short clips, PRVR employs untrimmed long videos where the content is only partially relevant to text queries.

TVR is collected from six TV shows, containing 21.8K videos and 109K text queries. Each video has five textual descriptions on average, depicting different moments in the video. Following [8],

the training set consists of 17,435 videos with 87,175 moments, while the test set contains 2,179 videos with 10,895 moments.

ActivityNet Captions consists of a wide range of human activities, sourced from 20K YouTube videos. On average, each video has 3.7 moments with sentence descriptions. We adopt the same data partition as in [8, 13, 40], where 10,009 and 4,917 videos (37,421 and 17,505 moments) are utilized as the training and test sets.

Charades-STA primarily comprises videos that depict indoor activities, including 6,670 videos and 16,128 moment annotations. We utilize the official data partition, 12,408 and 3,720 moment-sentence pairs for training and evaluation, respectively.

4.1.2 Evaluation Metrics. Following previous works [8, 13, 40], we adopt the rank-based metrics Recall Rate at k ($R@k$) and the sum of all recall rates (SumR). $R@k$ measures the proportion of relevant items successfully retrieved within the top- k results, with k set to $\{1, 5, 10, 100\}$. Higher recall rates indicate better retrieval accuracy.

4.1.3 Implementation Details. To ensure a fair comparison with previous works on PRVR [8, 13, 19, 40, 44], we utilize the same visual and textual features provided by [8]. The visual and textual features are extracted by pre-trained I3D [4] and RoBERTa [30], respectively. The feature dimension D is set to 384. T_m , m , and α are set to 32, 0.2, and 0.7 following [8, 40]. β_t and β_r are pre-defined as 0.4 and 0.25. g is set to 8. We set $\lambda_{\{1,2,3,4,5\}}$ to $\{0.02, 0.04, 0.1, 1, 1\}$. For model training, we utilize the Adam optimizer [21] with an initial learning rate of $2.5e-4$ and a mini-batch size of 128. The model is trained for 100 epochs with an early stopping strategy. Dropout [35] is set to 0.15 to prevent overfitting. All experiments are conducted on a single NVIDIA RTX 3090 GPU.

4.2 Comparison with State-of-the-Arts

We compare the proposed method with other state-of-the-art methods on TVR, ActivityNet Captions, and Charades-STA. These methods consist of both PRVR and T2VR models. The results are borrowed from [8, 40] and the reported results of corresponding papers.

Table 2: Main ablation studies of the proposed key modules on Charades-STA. The best results are in bold.

Row	Setting			R@1	R@5	R@10	R@100	SumR
	ICE	IRM	TCP					
1	✗	✗	✗	1.5	6.8	11.3	49.5	69.1
2	✓	✗	✗	2.2	7.5	12.4	52.2	74.3
3	✗	✓	✗	2.1	7.8	12.9	51.9	74.7
4	✗	✗	✓	1.7	7.0	12.0	50.5	71.2
5	✗	✓	✓	2.4	8.3	13.8	52.1	76.6
6	✓	✗	✓	2.5	8.5	13.6	52.2	76.8
7	✓	✓	✗	2.6	8.8	14.2	52.6	78.2
8	✓	✓	✓	2.9	9.2	14.9	54.3	81.3

Table 3: Ablation study of loss terms in the Intra Redundancy Mining module on Charades-STA.

Row	Loss Terms		R@1	R@5	R@10	R@100	SumR
	\mathcal{L}_{neg}	\mathcal{L}_{red}					
1	✗	✗	2.5	8.5	13.6	52.2	76.8
2	✓	✗	2.3	8.9	14.9	53.2	79.3
3	✗	✓	2.3	8.7	14.7	52.8	78.5
4	✓	✓	2.9	9.2	14.9	54.3	81.3

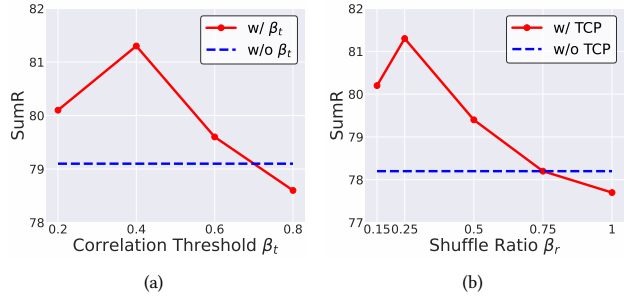
As summarized in Table 1, our method achieves state-of-the-art (SOTA) performance on all three datasets across all metrics. Specifically, we achieve significant improvements in SumR across these benchmarks: (1) On the TVR dataset, we outperform the previous SOTA method DL-DKD [13] by 14.1% absolute and 7.84% relative improvements. (2) On ActivityNet Captions, we surpass DL-DKD with gains of 12.8% absolute and 8.67% relative improvements. (3) On Charades-STA, we exceed PEAN [19] by 6.6% absolute and 8.84% relative improvements. These results demonstrate the effectiveness and robustness of our approach.

4.3 Ablation Study

4.3.1 Main Ablation Studies. To comprehensively validate the effectiveness of each module in our method, we conduct extensive ablation studies in Table 2. In particular, Row 1 indicates the base model trained with \mathcal{L}_{base} only, whose retrieval accuracy is far below the full model (Row 8) trained with Equation (13). Comparing the results in each row, we have the following observations:

(1) Each module independently improves performance over the base model (Row 1). The ICE module (Row 2) boosts SumR by 5.2, demonstrating its ability to enhance inter-sample semantic alignment. The IRM module (Row 3) improves SumR by 5.6, indicating its role in refining the cross-modal semantic space. The TCP module (Row 4) achieves the gain of 2.1 in SumR, highlighting its effectiveness in learning discriminative visual features.

(2) Combining any two modules yields further improvements (Row 5-7), indicating their complementary roles in aligning semantics. Specifically, the joint application of ICE and IRM achieves the

**Figure 5: Ablation study of the correlation threshold β_t in the Inter Correlation Enhancement module and the shuffle ratio β_r in the Temporal Coherence Prediction module.**

largest gain (Row 7), highlighting the necessity of exploiting the cross-modal dual nature of video-text modalities in PRVR.

(3) Integrating all three modules leads to the best performance (Row 8), with significant gains across all metrics. This proves the effectiveness of jointly leveraging inter-sample correlations, intra-sample redundancy mining, and temporal coherence learning.

4.3.2 Inter Correlation Enhancement. We validate the efficacy of the correlation threshold β_t in the Inter Correlation Enhancement module. As presented in Figure 5 (a), the choice of β_t affects retrieval performance. When β_t is set to 0.4, the model achieves the highest SumR of 81.3, outperforming both lower and higher thresholds. Lowering β_t to 0.2 increases noise from weakly correlated pairs, reducing SumR to 80.1. On the other hand, raising β_t to 0.6 or 0.8 over-suppresses potential correlations, thus degrading SumR to 79.6 and 78.6, respectively. Notably, the absence of β_t (i.e., retaining all candidate pairs) yields a suboptimal SumR of 79.1, demonstrating that indiscriminate inclusion of low-similarity pairs could introduce harmful noise during training.

4.3.3 Intra Redundancy Mining. We investigate the effectiveness of each loss function and their combinations in the Intra Redundancy Mining (IRM) module. As shown in Table 3, both \mathcal{L}_{neg} (Row 2) and \mathcal{L}_{red} (Row 3) lead to improvements across all metrics. Moreover, combining \mathcal{L}_{neg} and \mathcal{L}_{red} yields the highest SumR, outperforming either loss alone. The effectiveness arises because \mathcal{L}_{neg} directly suppresses redundancy by pushing away hard negatives, while \mathcal{L}_{red} implicitly strengthens cross-modal alignment by correlating video-view and query-view redundancies.

4.3.4 Temporal Coherence Prediction. We assess the impact of the shuffle ratio β_r in the Temporal Coherence Prediction (TCP) module. As illustrated in Figure 5 (b), the choice of β_r influences the model's ability to learn temporal coherence. When $\beta_r = 0.25$, the model achieves the optimal SumR of 81.3, outperforming all other configurations. Adopting other ratios results in degradations in performance: smaller ratios yield insufficient learning signals, as minimal shuffling fails to challenge the model's temporal reasoning. Conversely, larger ratios excessively disrupt temporal coherence, making the reordering task overly ambiguous and harming feature learning. Notably, the worst β_r configuration even underperforms the full absence of TCP, demonstrating the necessity of setting a proper shuffle ratio.

Table 4: Ablation study of the Temporal Coherence Prediction module on Charades-STA.

Row	Setting		R@1	R@5	R@10	R@100	SumR
	Video	Moment					
1	✗	✗	2.6	8.8	14.2	52.6	78.2
2	✓	✗	2.7	9.0	14.6	53.4	79.7
3	✗	✓	2.8	8.9	14.8	53.7	80.2
4	✓	✓	2.9	9.2	14.9	54.3	81.3

Table 5: Effect on different base models on Charades-STA. We directly apply our proposed three modules to existing PRVR methods.

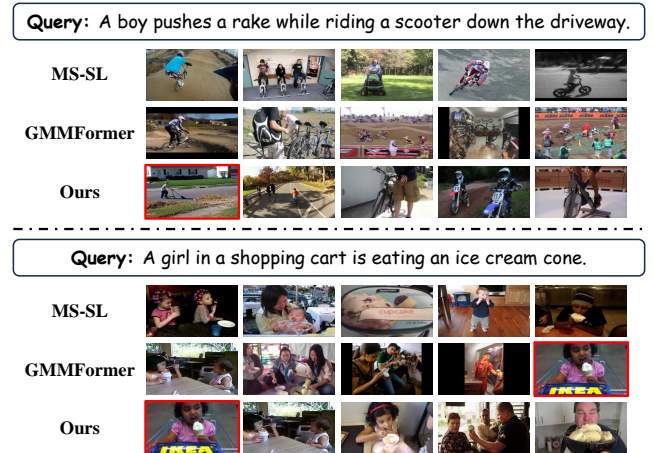
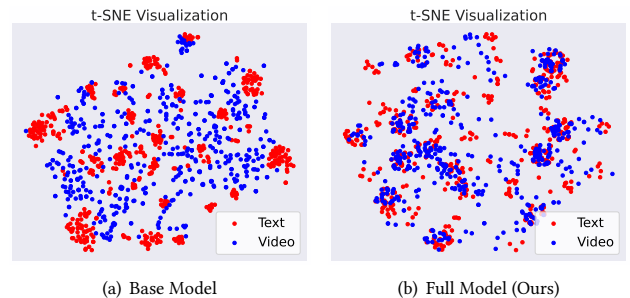
Method	Setting	R@1	R@5	R@10	R@100	SumR
MS-SL [8]	Origin	1.8	7.1	11.8	47.7	68.4
	+ Ours	2.4	9.1	14.6	53.9	80.0
GMMFormer [40]	Origin	2.1	7.8	12.5	50.6	72.9
	+ Ours	3.0	9.5	15.3	55.1	82.9

We then demonstrate the contribution of applying the TCP module to both the video-level branch and the moment-level branch. As depicted in Table 4, leveraging TCP solely on the video-level branch (Row 2) improves SumR to 79.7, primarily enhancing fine-grained temporal modeling. Besides, applying TCP only to the moment-level branch (Row 3) achieves an improved SumR of 80.2, as moment-level coherence learning encourages the encoder to reason coarse-grained temporal relationships. Furthermore, the full setup (Row 4) integrates these advantages, achieving the best performance across all metrics. This dual-branch design ensures holistic temporal coherence learning at multiple granularities, which is essential for robust temporal feature learning.

4.3.5 Base Model. To demonstrate the broader generalization of our method, we further integrate it into two existing PRVR models: MS-SL [8] and GMMFormer [40]. Concretely, we directly replace the base model with these models. As shown in Table 5, our approach acts as a plug-and-play enhancement to these models on the Charades-STA dataset. Consistent performance improvements are observed across both models. For instance, our method boosts SumR by 16.96% for MS-SL and 13.72% for GMMFormer in relative improvements, demonstrating its effectiveness and generalization. These results suggest that existing PRVR models inherently suffer from the limited cross-modal alignment. In contrast, our method systematically exploits the inter-sample correlation and intra-sample redundancy, resulting in substantial performance improvements. The universal gains also highlight that our method is model-agnostic and effectively constructs a more comprehensive cross-modal semantic space.

4.4 Qualitative Results

4.4.1 Retrieval Results. To qualitatively validate the effectiveness of our method, we report visualization comparisons of retrieval

**Figure 6: Visualization comparisons of retrieval results between our method, MS-SL [8], and GMMFormer [40] on ActivityNet Captions. Top-5 retrieval results are shown from left to right. Ground-truth videos are marked with red boxes. Zoom in for better visibility.****Figure 7: t-SNE visualization [36] of text and video features on Charades-STA. (a) is the base model trained with only \mathcal{L}_{base} . (b) shows the full model trained with Equation (13).**

results between our method, MS-SL [8], and GMMFormer [40] on ActivityNet Captions in Figure 6. In the first case, MS-SL and GMMFormer superficially match videos with the action *riding* and mistakenly associate *riding* with *bikes*, ignoring key semantics including *pushes a rake* and *scooter*. In contrast, our method accurately retrieves the target video with correct semantics. The remaining example also shows a similar phenomenon, which demonstrates the robust and superior retrieval capability of our method.

4.4.2 t-SNE Visualization. We report t-SNE visualization [36] to analyze the alignment of video and text features in the semantic space. For clearer observation, we randomly sample a subset of paired videos and text queries from Charades-STA. As shown in Figure 7 (a), in the base model, the distributions of video and text features exhibit limited overlap in the shared cross-modal space, indicating weak alignment between the two modalities. In contrast, our method achieves a more discriminative feature distribution. As in Figure 7 (b), video and text features are tightly interleaved in regions and the regions maintain sufficient separation to preserve

semantics-specific distinctions. This suggests that our approach successfully aligns the two modalities while retaining their unique characteristics, leading to improved semantic alignment for PRVR.

5 Conclusion

In this paper, we present a novel framework for Partially Relevant Video Retrieval, which systematically exploits the cross-modal nature of video-text modalities: inter-sample correlation and intra-sample redundancy. Our approach introduces three key modules. The Inter Correlation Enhancement module strengthens cross-modal alignment by identifying and leveraging semantically similar yet unpaired text-video samples as pseudo-positive pairs. The Intra Redundancy Mining module improves discriminative learning by treating redundant video moments as hard negative samples, forcing the model to focus on query-relevant visual semantics. The Temporal Coherence Prediction module enhances temporal feature discrimination through a self-supervised video sequence prediction task. Extensive experiments on three datasets demonstrate that our framework achieves state-of-the-art performance.

References

- [1] Dzmitry Bahdanau, Kyunghyun Cho, and Yoshua Bengio. 2015. Neural machine translation by jointly learning to align and translate. In *3rd International Conference on Learning Representations*.
- [2] Meng Cao, Long Chen, Mike Zheng Shou, Can Zhang, and Yuexian Zou. 2021. On Pursuit of Designing Multi-modal Transformer for Video Grounding. In *Proceedings of the 2021 Conference on Empirical Methods in Natural Language Processing*. 9810–9823.
- [3] Nicolas Carion, Francisco Massa, Gabriel Synnaeve, Nicolas Usunier, Alexander Kirillov, and Sergey Zagoruyko. 2020. End-to-end object detection with transformers. In *European conference on computer vision*. Springer, 213–229.
- [4] Joao Carreira and Andrew Zisserman. 2017. Quo vadis, action recognition? a new model and the kinetics dataset. In *Proceedings of the IEEE Conference on Computer Vision and Pattern Recognition*. 6299–6308.
- [5] David Chen and William B Dolan. 2011. Collecting highly parallel data for paraphrase evaluation. In *Proceedings of the 49th annual meeting of the association for computational linguistics: human language technologies*. 190–200.
- [6] Shizhe Chen, Yida Zhao, Qin Jin, and Qi Wu. 2020. Fine-grained video-text retrieval with hierarchical graph reasoning. In *Proceedings of the IEEE/CVF conference on computer vision and pattern recognition*. 10638–10647.
- [7] Zhiguo Chen, Xun Jiang, Xing Xu, Zuo Cao, Yijun Mo, and Heng Tao Shen. 2023. Joint Searching and Grounding: Multi-Granularity Video Content Retrieval. In *Proceedings of the 31st ACM International Conference on Multimedia*. 975–983.
- [8] Jianfeng Dong, Xianke Chen, Minsong Zhang, Xun Yang, Shujie Chen, Xirong Li, and Xun Wang. 2022. Partially Relevant Video Retrieval. In *Proceedings of the 30th ACM International Conference on Multimedia*. 246–257.
- [9] Jianfeng Dong, Xirong Li, Chaoxi Xu, Shouling Ji, Yuan He, Gang Yang, and Xun Wang. 2019. Dual encoding for zero-example video retrieval. In *Proceedings of the IEEE/CVF conference on computer vision and pattern recognition*. 9346–9355.
- [10] Jianfeng Dong, Xirong Li, Chaoxi Xu, Xun Yang, Gang Yang, Xun Wang, and Meng Wang. 2021. Dual encoding for video retrieval by text. *IEEE Transactions on Pattern Analysis and Machine Intelligence* 44, 8 (2021), 4065–4080.
- [11] Jianfeng Dong, Xiaoman Peng, Daizong Liu, Xiaoye Qu, Xun Yang, Cuizhu Bao, and Meng Wang. 2024. Temporal Sentence Grounding with Relevance Feedback in Videos. *Advances in Neural Information Processing Systems* 37 (2024), 43107–43132.
- [12] Jianfeng Dong, Yabing Wang, Xianke Chen, Xiaoye Qu, Xirong Li, Yuan He, and Xun Wang. 2022. Reading-strategy inspired visual representation learning for text-to-video retrieval. *IEEE transactions on circuits and systems for video technology* 32, 8 (2022), 5680–5694.
- [13] Jianfeng Dong, Minsong Zhang, Zheng Zhang, Xianke Chen, Daizong Liu, Xiaoye Qu, Xun Wang, and Baolong Liu. 2023. Dual Learning with Dynamic Knowledge Distillation for Partially Relevant Video Retrieval. In *Proceedings of the IEEE/CVF International Conference on Computer Vision*. 11302–11312.
- [14] Fartash Faghri, David J Fleet, Jamie Ryan Kiros, and Sanja Fidler. 2018. VSE++: Improving Visual-Semantic Embeddings with Hard Negatives. In *Proceedings of the British Machine Vision Conference (BMVC)*.
- [15] Xiang Fang, Wanlong Fang, Daizong Liu, Xiaoye Qu, Jianfeng Dong, Pan Zhou, Renfu Li, Zichuan Xu, Lixing Chen, Panpan Zheng, et al. 2024. Not all inputs are valid: Towards open-set video moment retrieval using language. In *Proceedings of the 32nd ACM International Conference on Multimedia*. 28–37.
- [16] Jiyang Gao, Chen Sun, Zhenheng Yang, and Ram Nevatia. 2017. Tall: Temporal activity localization via language query. In *Proceedings of the IEEE international conference on computer vision*. 5267–5275.
- [17] Jiachang Hao, Haifeng Sun, Pengfei Ren, Jingyu Wang, Qi Qi, and Jianxin Liao. 2022. Query-aware video encoder for video moment retrieval. *Neurocomputing* 483 (2022), 72–86.
- [18] Zhijian Hou, Chong-Wah Ngo, and Wing Kwong Chan. 2021. Conquer: Contextual query-aware ranking for video corpus moment retrieval. In *Proceedings of the 29th ACM International Conference on Multimedia*. 3900–3908.
- [19] Xun Jiang, Zhiguo Chen, Xing Xu, Fumin Shen, Zuo Cao, and Xunliang Cai. 2023. Progressive Event Alignment Network for Partially Relevant Video Retrieval. In *2023 IEEE International Conference on Multimedia and Expo (ICME)*. IEEE, 1973–1978.
- [20] Minjoon Jung, Youwon Jang, Seongho Choi, Joochan Kim, Jin-Hwa Kim, and Byoung-Tak Zhang. 2025. Background-Aware Moment Detection for Video Moment Retrieval. In *Proceedings of the Winter Conference on Applications of Computer Vision (WACV)*. 8575–8585.
- [21] Diederik P. Kingma and Jimmy Ba. 2015. Adam: A Method for Stochastic Optimization. In *3rd International Conference on Learning Representations*.
- [22] Ranjay Krishna, Kenji Hata, Frederic Ren, Li Fei-Fei, and Juan Carlos Niebles. 2017. Dense-captioning events in videos. In *Proceedings of the IEEE international conference on computer vision*. 706–715.
- [23] Jie Lei, Tamara L Berg, and Mohit Bansal. 2021. Detecting moments and highlights in videos via natural language queries. *Advances in Neural Information Processing Systems* 34 (2021), 11846–11858.
- [24] Jie Lei, Licheng Yu, Tamara L Berg, and Mohit Bansal. 2020. Tvr: A large-scale dataset for video-subtitle moment retrieval. In *Computer Vision—ECCV 2020: 16th European Conference, Glasgow, UK, August 23–28, 2020, Proceedings, Part XXI*. Springer, 447–463.
- [25] Kunchang Li, Yali Wang, Yizhuo Li, Yi Wang, Yinan He, Limin Wang, and Yu Qiao. 2023. Unmasked teacher: Towards training-efficient video foundation models. In *Proceedings of the IEEE/CVF International Conference on Computer Vision*. 19948–19960.
- [26] Xirong Li, Chaoxi Xu, Gang Yang, Zhineng Chen, and Jianfeng Dong. 2019. W2vv++ fully deep learning for ad-hoc video search. In *Proceedings of the 27th ACM international conference on multimedia*. 1786–1794.
- [27] Kevin Qinghong Lin, Pengchuan Zhang, Joya Chen, Shraman Pramanick, Difei Gao, Alex Jinpeng Wang, Rui Yan, and Mike Zheng Shou. 2023. Univt: Towards unified video-language temporal grounding. In *Proceedings of the IEEE/CVF International Conference on Computer Vision*. 2794–2804.
- [28] Daizong Liu, Xiang Fang, Wei Hu, and Pan Zhou. 2023. Exploring optical-flow-guided motion and detection-based appearance for temporal sentence grounding. *IEEE Transactions on Multimedia* (2023).
- [29] Ye Liu, Siyuan Li, Yang Wu, Chang-Wen Chen, Ying Shan, and Xiaohu Qie. 2022. Umt: Unified multi-modal transformers for joint video moment retrieval and highlight detection. In *Proceedings of the IEEE/CVF Conference on Computer Vision and Pattern Recognition*. 3042–3051.
- [30] Yinhan Liu, Myle Ott, Naman Goyal, Jingfei Du, Mandar Joshi, Danqi Chen, Omer Levy, Mike Lewis, Luke Zettlemoyer, and Veselin Stoyanov. 2019. Roberta: A robustly optimized bert pretraining approach. *arXiv preprint arXiv:1907.11692* (2019).
- [31] Chujie Lu, Long Chen, Chilie Tan, Xiaolin Li, and Jun Xiao. 2019. Debug: A dense bottom-up grounding approach for natural language video localization. In *Proceedings of the 2019 Conference on Empirical Methods in Natural Language Processing and the 9th International Joint Conference on Natural Language Processing (EMNLP-IJCNLP)*. 5144–5153.
- [32] WonJun Moon, Sangeek Hyun, SangUk Park, Dongchan Park, and Jae-Pil Heo. 2023. Query-dependent video representation for moment retrieval and highlight detection. In *Proceedings of the IEEE/CVF Conference on Computer Vision and Pattern Recognition*. 23023–23033.
- [33] Aaron van den Oord, Yazhe Li, and Oriol Vinyals. 2018. Representation learning with contrastive predictive coding. *arXiv preprint arXiv:1807.03748* (2018).
- [34] Alec Radford, Jong Wook Kim, Chris Hallacy, Aditya Ramesh, Gabriel Goh, Sandhini Agarwal, Girish Sastry, Amanda Askell, Pamela Mishkin, Jack Clark, et al. 2021. Learning transferable visual models from natural language supervision. In *International conference on machine learning*. PMLR, 8748–8763.
- [35] Nitish Srivastava, Geoffrey Hinton, Alex Krizhevsky, Ilya Sutskever, and Ruslan Salakhutdinov. 2014. Dropout: a simple way to prevent neural networks from overfitting. *The journal of machine learning research* 15, 1 (2014), 1929–1958.
- [36] Laurens van der Maaten and Geoffrey Hinton. 2008. Visualizing Data using t-SNE. *Journal of Machine Learning Research* 9, 86 (2008), 2579–2605. <http://jmlr.org/papers/v9/vandermaten08a.html>
- [37] Ashish Vaswani, Noam Shazeer, Niki Parmar, Jakob Uszkoreit, Llion Jones, Aidan N Gomez, Łukasz Kaiser, and Illia Polosukhin. 2017. Attention is all you need. *Advances in neural information processing systems* 30 (2017).

- [38] Xin Wang, Jiawei Wu, Junkun Chen, Lei Li, Yuan-Fang Wang, and William Yang Wang. 2019. Vatex: A large-scale, high-quality multilingual dataset for video-and-language research. In *Proceedings of the IEEE/CVF international conference on computer vision*. 4581–4591.
- [39] Yi Wang, Kunchang Li, Xinhao Li, Jiashuo Yu, Yinan He, Guo Chen, Baoqi Pei, Rongkun Zheng, Zun Wang, Yansong Shi, et al. 2024. Internvideo2: Scaling foundation models for multimodal video understanding. In *European Conference on Computer Vision*. Springer, 396–416.
- [40] Yuting Wang, Jinpeng Wang, Bin Chen, Ziyun Zeng, and Shu-Tao Xia. 2024. GMMFormer: Gaussian-Mixture-Model Based Transformer for Efficient Partially Relevant Video Retrieval. In *Proceedings of the AAAI Conference on Artificial Intelligence*.
- [41] Zhenzhi Wang, Limin Wang, Tao Wu, Tianhao Li, and Gangshan Wu. 2022. Negative sample matters: A renaissance of metric learning for temporal grounding. In *Proceedings of the AAAI Conference on Artificial Intelligence*, Vol. 36. 2613–2623.
- [42] Wenhao Wu, Haipeng Luo, Bo Fang, Jingdong Wang, and Wanli Ouyang. 2023. Cap4video: What can auxiliary captions do for text-video retrieval?. In *Proceedings of the IEEE/CVF conference on computer vision and pattern recognition*. 10704–10713.
- [43] Jun Xu, Tao Mei, Ting Yao, and Yong Rui. 2016. Msr-vtt: A large video description dataset for bridging video and language. In *Proceedings of the IEEE conference on computer vision and pattern recognition*. 5288–5296.
- [44] Shukang Yin, Sirui Zhao, Hao Wang, Tong Xu, and Enhong Chen. 2024. Exploiting Instance-level Relationships in Weakly Supervised Text-to-Video Retrieval. *ACM Transactions on Multimedia Computing, Communications and Applications* 20, 10 (2024), 1–21.
- [45] Yitian Yuan, Lin Ma, Jingwen Wang, Wei Liu, and Wenwu Zhu. 2019. Semantic conditioned dynamic modulation for temporal sentence grounding in videos. *Advances in Neural Information Processing Systems* 32 (2019).
- [46] Hao Zhang, Aixin Sun, Wei Jing, Guoshun Nan, Liangli Zhen, Joey Tianyi Zhou, and Rick Siow Mong Goh. 2021. Video corpus moment retrieval with contrastive learning. In *Proceedings of the 44th International ACM SIGIR Conference on Research and Development in Information Retrieval*. 685–695.
- [47] Hao Zhang, Aixin Sun, Wei Jing, and Joey Tianyi Zhou. 2020. Span-based Localizing Network for Natural Language Video Localization. In *Proceedings of the 58th Annual Meeting of the Association for Computational Linguistics*. 6543–6554.
- [48] Songyang Zhang, Houwen Peng, Jianlong Fu, and Jiebo Luo. 2020. Learning 2d temporal adjacent networks for moment localization with natural language. In *Proceedings of the AAAI Conference on Artificial Intelligence*, Vol. 34. 12870–12877.
- [49] Zongmeng Zhang, Xianjing Han, Xuemeng Song, Yan Yan, and Liqiang Nie. 2021. Multi-modal interaction graph convolutional network for temporal language localization in videos. *IEEE Transactions on Image Processing* 30 (2021), 8265–8277.
- [50] Minghang Zheng, Sizhe Li, Qingchao Chen, Yuxin Peng, and Yang Liu. 2023. Phrase-level temporal relationship mining for temporal sentence localization. In *Proceedings of the AAAI Conference on Artificial Intelligence*, Vol. 37. 3669–3677.
- [51] Hao Zhou, Chongyang Zhang, Yan Luo, Yanjun Chen, and Chuanping Hu. 2021. Embracing uncertainty: Decoupling and de-bias for robust temporal grounding. In *Proceedings of the IEEE/CVF Conference on Computer Vision and Pattern Recognition*. 8445–8454.